

See discussions, stats, and author profiles for this publication at: <https://www.researchgate.net/publication/262148824>

# A Comparative Study of Protein Unfolding in Aqueous Urea and DMSO Solutions: Surface Polarity, Solvent Specificity and Sequence of Secondary Structure Melting.

ARTICLE *in* THE JOURNAL OF PHYSICAL CHEMISTRY B · MAY 2014

Impact Factor: 3.3 · DOI: 10.1021/jp5037348 · Source: PubMed

---

CITATIONS

3

---

READS

40

## 2 AUTHORS:



Susmita Roy

Rice University

23 PUBLICATIONS 164 CITATIONS

SEE PROFILE



Biman Bagchi

Indian Institute of Science

456 PUBLICATIONS 10,995 CITATIONS

SEE PROFILE

# Comparative Study of Protein Unfolding in Aqueous Urea and Dimethyl Sulfoxide Solutions: Surface Polarity, Solvent Specificity, and Sequence of Secondary Structure Melting

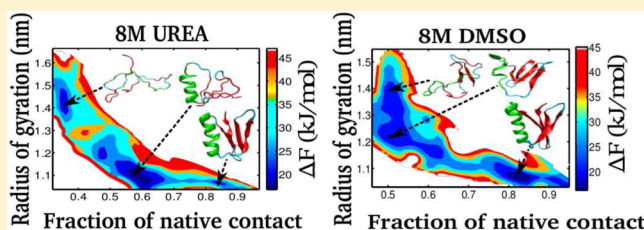
Susmita Roy and Biman Bagchi\*

Solid State and Structural Chemistry Unit, Indian Institute of Science, Bangalore 560012, India

**S** Supporting Information

**ABSTRACT:** Elucidation of possible pathways between folded (native) and unfolded states of a protein is a challenging task, as the intermediates are often hard to detect. Here, we alter the solvent environment in a controlled manner by choosing *two different cosolvents* of water, urea, and dimethyl sulfoxide (DMSO) and study unfolding of *four different proteins* to understand the respective sequence of melting by computer simulation methods. We indeed find interesting differences in the sequence of melting of  $\alpha$  helices and  $\beta$  sheets

in these two solvents. For example, in 8 M urea solution,  $\beta$ -sheet parts of a protein are found to unfold preferentially, followed by the unfolding of  $\alpha$  helices. In contrast, 8 M DMSO solution unfolds  $\alpha$  helices first, followed by the separation of  $\beta$  sheets for the majority of proteins. Sequence of unfolding events in four different  $\alpha/\beta$  proteins and also in chicken villin head piece (HP-36) both in urea and DMSO solutions demonstrate that the unfolding pathways are determined jointly by relative exposure of polar and nonpolar residues of a protein and the mode of molecular action of a solvent on that protein.



## 1. INTRODUCTION

Mechanism of folding/unfolding of different proteins under different environments is a highly complex physicochemical process that is yet to be fully understood. A native state of protein is stabilized and held together in aqueous environments by variety of forces, such as hydrogen bonding and hydrophobic attraction among amino acid residues.<sup>1</sup> The nature of these forces is different. While hydrogen bonding is pair specific, hydrophobic force is more collective and gets enhanced in an aggregate.<sup>1</sup> These forces together determine the pathways of folding and unfolding in a given environment. Thus, the pathway can change as the environment changes, and this is an important aspect of the protein folding problem.

The folding funnel paradigm with its associated energy landscape view has been applied to find a general semi-quantitative approach to rationalize a vast amount of information available now.<sup>2–21</sup> A major prediction of the folding funnel paradigm is the existence of multiple pathways during transition from the folded to the unfolded state and vice versa, and in the process, a protein is predicted to evolve through different intermediate states. This prediction has been a subject of intense debate with examples both in favor and in opposition.<sup>2–26</sup> The issue is still far from settled. It is indeed a daunting task to map out the full folding pathway at an atomic level. One possible approach is to use different chemical denaturants in the hope of finding different pathways of unfolding.<sup>5–8</sup> Early work of Bennion and Daggett demonstrated for chymotrypsin inhibitor-2 that, in 8 M urea solution, the  $\beta$  structure melts first, followed by  $\alpha$  helix.<sup>27</sup> In similar recent studies, Rocco and co-workers compared the unfolding

pathways of protein L in different denaturation modes, such as temperature, urea, and guanidinium chloride.<sup>28,29</sup> They reported that, in 10 M urea,  $\beta$  sheet is destabilized first, whereas in temperature and 5 M GdmCl, it is the  $\alpha$  helix. Englander and co-workers carried out a series of unfolding studies and concluded that unfolding follows a definite predetermined pathway.<sup>30–32</sup> Fayer and co-workers found the system to settle in a molten globule state.<sup>33</sup> For urea-mediated denaturation, two mechanisms have been proposed: (i) an indirect mechanism where urea drags out the hydrogen-bound water molecules by dehydrating the protein surface that indirectly facilitates the unfolding event;<sup>34</sup> and (ii) a direct mechanism where urea preferentially binds with protein molecules through a strong dispersion interaction competing with water.<sup>35,36</sup>

The fact that most of the recent theoretical and molecular dynamics (MD) simulations employ urea and guanidine chloride as denaturing solvents has somewhat limited our data pool;<sup>27–29,34–40</sup> examples of the use of other cosolvent-induced protein unfolding are sparse. Among those cosolvents, dimethyl sulfoxide (DMSO) is unique.<sup>41–44</sup> It is popularly used as a stock solution in drug discovery processes and efficiently plays roles as a stabilizer, an activator, an inhibitor, a cryoprotector, and a capable denaturant. While at low concentrations of DMSO ( $X_{\text{DMSO}} < 0.05$ ) the majority of proteins are found to be conformationally unaffected, they

Received: April 16, 2014

Revised: April 28, 2014

Published: May 7, 2014

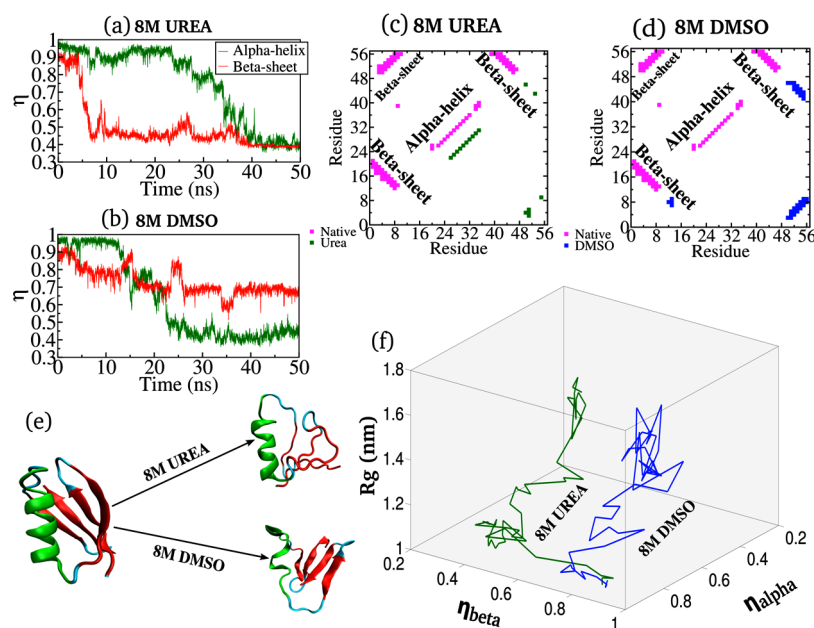


**Figure 1.** Fraction of native contact ( $\eta$ ) dynamics of protein G, in (a) 8 M urea and (b) 8 M DMSO solutions. Contact map of protein G at intermediate simulation time frame (20 ns) in (c) 8 M urea and (d) 8 M DMSO. (e) Snapshot of two different intermediates obtained from urea- and DMSO-induced unfolding trajectories. (f) Conformational degrees of freedom of the protein along the fraction of  $\beta$ -sheet native contact ( $x$  axis:  $\eta_{\beta}$ ), the fraction of  $\alpha$ -helix native contact ( $y$  axis:  $\eta_{\alpha}$ ), and along the radius of gyration ( $z$  axis:  $R_g$ ) at their explicit time.

undergo a number of structural changes as DMSO concentration increases. We recently carried out studies aimed at understanding the quite different molecular interaction that DMSO provides between a protein and its chemical environment.<sup>41</sup> Along with our early studies, many other research groups also found the sensitivity of secondary structure of protein upon aqueous DMSO treatment.<sup>41–45</sup> Very recently, from Raman optical activity measurements, Blanch and co-workers found DMSO to selectively act on  $\alpha$  helices for a number of proteins at higher DMSO mole fraction whereas  $\beta$  sheets remained unaffected regardless of solvent concentration.<sup>46</sup> All these works greatly motivate us to examine the capability of DMSO as a helix breaker and the origin of its selectivity at a molecular level.

In the present work, we study and compare the unfolding of four proteins using different denaturing conditions, specifically in various concentrations of aqueous urea and aqueous DMSO solutions. This allows us to quantify the sensitivity of different secondary structural segments of a particular protein toward addition of such cosolvents. In addition, we selectively choose those proteins where the two principal secondary structural contents, that is,  $\alpha$  helix and  $\beta$  sheet, are present in their native conformation. Unfolding of four such well-characterized  $\alpha/\beta$  proteins, namely, (1) single immunoglobulin-binding domain protein G (PDB ID: 1GB1) from group G *Streptococcus*, (2) chymotrypsin inhibitor 2 (PDB ID: 2CI2), (3) IgG-binding domain of protein L (PDB ID: 2PTL), and (4) human erythrocytic ubiquitin (PDB ID: 1UBQ), were studied both in aqueous urea and DMSO solutions by the MD simulation method. We also studied chicken villin head piece HP-36 earlier, but that has only helices.<sup>44</sup> The details of the MD simulation technique are described in the System Setup and Simulation Details section.

## 2. SOLVENT SENSITIVITY OF SECONDARY STRUCTURES IN 8 M UREA AND 8 M DMSO

**2.1. Differential Stability of  $\alpha$  Helices and  $\beta$  Sheets.** To characterize the effects of urea and DMSO on those selected proteins, we individually track the time progression of unfolding by following their conformational changes in the particular secondary structural segments. We observe that, quite generally, urea solution preferentially initiates unfolding of its  $\beta$ -sheet part of such  $\alpha/\beta$  proteins that is followed by unfolding of the  $\alpha$ -helical content. This is also in accordance with other simulation results.<sup>27–29</sup> In contrast, the 8 M DMSO solution initially unfolds  $\alpha$  helix and then  $\beta$  sheet, with lower priority. DMSO-induced such selective melting has also been observed by recent Raman optical activity measurements.<sup>46</sup> Figure 1 shows diverse effects of urea and DMSO on a single protein, GB1 (protein G). In Figure 1a, b, we display the time evolution of the fraction native contact ( $\eta$ ) exclusion/inclusion dynamics. In 8 M urea solution, while a considerable amount of correct native contact formation of the  $\beta$ -sheet segment is diminished within 10 ns of time scale (to  $\eta = 0.4$ ), that of the  $\alpha$  helix remains larger than 0.9 at the same time scale, which eventually starts to disappear a long time after (20 ns) the initial unfolding event. In 8 M DMSO solution, in contrast,  $\alpha$ -helical native contacts break faster than those of  $\beta$  sheet. Time progression up to 50 ns shows that the fraction of native contact ( $\eta$ ) decreases only up to 0.6 in the case of the  $\beta$ -sheet segment of protein G. The contact map analysis in the transition state of unfolding clearly provides the evidence of disappearance of  $\alpha$ -helical and  $\beta$ -sheet segments in 8 M DMSO and 8 M urea, respectively (see Figure 1c, d). The emergence of two different intermediates (as shown in Figure 1e) during the unfolding of protein G in 8 M urea and 8 M DMSO provides the most important evidence for the existence of two different denaturation pathways of unfolding. Conformational fluctuation of protein G in terms of root-mean-square fluctuation of  $\alpha$ -helix and  $\beta$ -sheet residues also show distinct behavior in 8 M

urea and 8 M DMSO (see Figure S1, Supporting Information). While destabilization phenomenon of secondary structures in terms of correct native contact arrangement dramatically differs for a specific protein in these two solvents, late-stage enhancement of radius of gyration ( $R_g$ ) remains a common event in the unfolding of protein G in any of these two solvents (see Figure 1f). This signifies the final splitting of tertiary structure that causes elongation of the whole polypeptide chain.

**2.2. Property-Based Free Energy Contours Detect Two Distinct Pathways.** To clearly demonstrate different unfolding trajectories, we derive a property-based free energy path contour of protein G during unfolding in 8 M urea and 8 M DMSO solutions (see Figure 2a, b). This contour plot shows

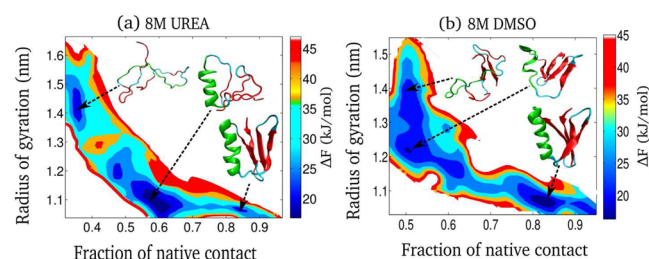


**Figure 2.** Radius of gyration ( $R_g$ ) and contact order parameter ( $\eta$ ) based free energy landscape along with relatively stable intermediates detected from the folding to unfolding transition of protein G in (a) 8 M urea and (b) 8 M DMSO solutions.

that the transition from native folded state to unfolded structure follows a minimum energy pathway evolving through different intermediates. It also provides the free energy separation between the folding and unfolding minima for both the two solvents. We could identify the ensemble of partially unfolded intermediates that are different in conformation and essentially bear the signature of different pathways in aqueous urea and DMSO solutions. It is worthwhile to note that unfolding by temperature and also by using GdmCl denaturants reveal diversity in the unfolding pathways of the structurally similar proteins.<sup>27–29</sup> Hence, one can surmise that the protein unfolding steps under any denaturing condition proceeds by following a specific minimum energy path that appears to be dominant among the multiple pathways of unfolding. That dominant route however might differ depending on the mode of denaturation.

**2.3. Molecular Mechanism of Urea- and DMSO-Induced Unfolding Processes.** To study the microscopic mechanism responsible for the emergence of such diverse unfolding events in urea and DMSO, we track their molecular interaction with proteins. In urea, due to the presence of more hydrophilic ends ( $C=O$  and two  $NH_2$ ), there is high propensity of forming hydrogen bonds with the side-chain residues and the backbone of  $\beta$  sheet, leading to the preferential binding with  $\beta$  sheets than  $\alpha$  helices (see Figure 3a). The molecular mechanism of DMSO-induced unfolding process is entirely different. It can be attributed to the preferential solvation of the hydrophobic side-chain atoms through the methyl groups of DMSO (see Figure 3b), followed by the hydrogen bonding of the oxygen atom of DMSO to the exposed backbone NH groups of protein G (see Figure 3c). It is important to note that  $\alpha$  helix of protein G has a relatively large hydrophobic solvent accessible surface area than that of  $\beta$  sheet. This accounts for the hydrophobic solvation through the

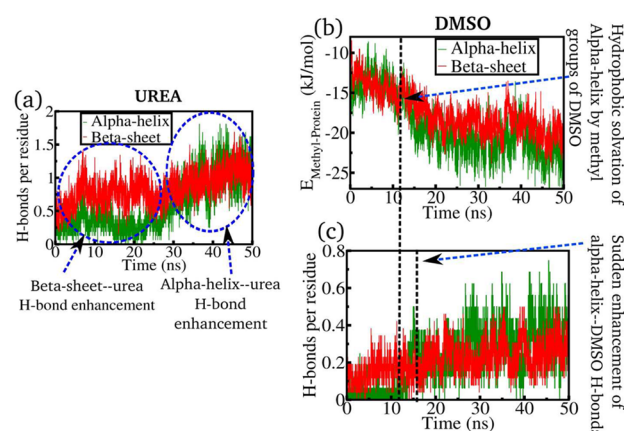


**Figure 3.** (a) Role of protein–urea hydrogen-bond interaction in elongation of  $\alpha$  helix and  $\beta$  sheet. (b) Role of the hydrophobic side chain–DMSO interaction and backbone–DMSO interaction underlying the unfolding mechanism.

methyl groups of DMSO leading to the fast melting of  $\alpha$  helices.

**2.4. Solvent Dependence of Unfolding Pathways for Other  $\alpha/\beta$  Proteins.** We have mentioned earlier that DMSO has attained less attention as a denaturant. To affirm the proposition of the microscopic unfolding mechanism induced by DMSO, we selectively study four such  $\alpha/\beta$  proteins including protein G. It also allows us to check whether they share similar unfolding pathways passing through the  $\alpha$  helix melted intermediate in 8 M DMSO. Combination of radius of gyration and the fraction of native contact dynamics (separately shown in Figure S2a–d, Supporting Information) in terms of their property-based free energy path shows that, similar to protein G, chymotrypsin inhibitor 2 and protein L also adopt the  $\alpha$  helix melted pathway (see Figure 4a–c). Exception still remains in the crowd. We find maximum unfolding trajectories of ubiquitin in DMSO do not proceed via the  $\alpha$  helix melted pathway (see Figure 4d).

**2.5. Mode of Action of a Solvent and Polar and Nonpolar Solvent Accessible Surface Area of a Protein together Determine the Dominant Route of Unfolding.** Recall that the DMSO-induced unfolding process is primarily governed by the preferential solvation of the hydrophobic side-chain atoms through the methyl groups of DMSO. To estimate the exposure of such side-chain atoms, we calculate the relative polar and nonpolar solvent accessible surface area (SASA) (estimates are given in Table 1) for each protein from their crystal structure that can be accessible for solvents we used. We find that all three proteins, namely, protein G, chymotrypsin inhibitor 2, and protein L, have relatively higher nonpolar surface exposure of their  $\alpha$ -helical content than the  $\beta$ -sheet content that actually leads to more effective hydrophobic interaction with the methyl groups of DMSO (see Table 1). In addition, the residual level analyses reveal that  $\alpha$  helix enriched with alanine residues also facilitate the  $\alpha$ -helix melting by preferential hydrophobic solvation. In comparison, ubiquitin has relatively less nonpolar surface exposure in its  $\alpha$ -helical segment that might be a dominant factor for choosing a selective unfolding route. This prerequisite information on surface polarity thus can provide immense information about the preferential unfolding pathway of a specific protein in a specific solvent if the molecular mechanism of protein–solvent interaction is already known.



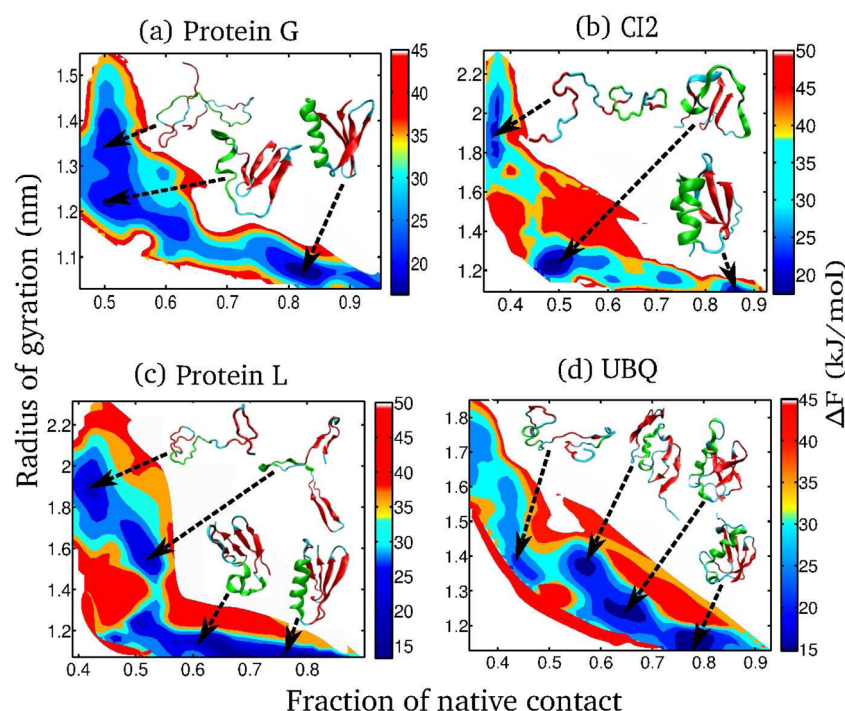


**Figure 4.** Radius of gyration ( $R_g$ ) and contact order parameter ( $\eta$ ) based free energy landscape along with relatively stable intermediates detected from the folding to unfolding transition of different proteins: (a) protein G, (b) chymotrypsin inhibitor 2 (CI2), (c) protein L, and (d) ubiquitin (UBQ) in 8 M DMSO solution.

**Table 1.** Relative Polar and Nonpolar SASA for the  $\alpha$ -Helix and  $\beta$ -Sheet of Four Proteins

	polar SASA		nonpolar SASA	
	$\alpha$ -helix	$\beta$ -sheet	$\alpha$ -helix	$\beta$ -sheet
protein G	39.30%	43.80%	60.70%	56.20%
chymotrypsin inhibitor 2	31.23%	40.61%	68.77%	59.39%
protein L	33.50%	40.75%	66.50%	59.25%
ubiquitin	44.30%	39.38%	55.70%	60.62%

### 3. CONCLUSION

While folding sequence is often dictated by the local “nativeness” of the unfolded state, there does not seem to exist such a general principle to predict the sequence of events unleashed during protein unfolding induced by chemical denaturants.<sup>47</sup> During unfolding, a long-lived kinetic intermediate can form by long-range intraresidual interactions<sup>48–50</sup> and also by apolar amino acid group–hydrophobic solvent interaction.<sup>47</sup> Such microscopic phenomena effectively dictate the course of unfolding.

Despite the well-known facts that both chemical and thermal denaturations unfold a protein, our understanding of the diversity of the unfolding mechanism at various environments has still remained at its infancy. Our MD simulations aim at elucidating the role of different molecular interactions between a protein and its environment that could assist in deciding the choice of a suitable solvent media in many experimental studies in enzymology and protein research. In this spirit, it is that we propose use of DMSO as a denaturant to melt helices preferentially.

Protein denaturation by aqueous urea gets initiated by the preferential solvation of the polar/charged hydrophilic residues on the protein surface by the polar head groups of urea. This leads to an effective repulsion between the residues on the

surface of proteins. As a result, protein swells, and its buried hydrophobic residues become exposed. These sequences of events match well with the early explanation reported by Thirumalai and co-workers.<sup>35</sup> In contrast, in aqueous DMSO, protein denaturation occurs by the combined effects of hydrophobic and hydrophilic interactions, *initiated first by the preferential solvation of the nonpolar amino acid residues on the protein surface by the methyl groups of DMSO*. Subsequently, the S=O bonds of DMSO pointing outward from the protein surface, form hydrogen bonds with water. This also gives rise to a swelling of the protein that in turn enhances the availability of backbone to further solvation. Then, the S=O groups of DMSO pull the backbone outward through hydrogen-bond interaction.

In the present context, for the majority of proteins,  $\alpha$ -helices have the larger hydrophobic surface exposure than that of  $\beta$  sheets, except ubiquitin. Hence, the majority of proteins choose *preferential hydrophobic solvation* of these helices as the unfolding pathway in DMSO. Our early observations and the current study suggest possible use of DMSO as an excellent helix breaker. On the other hand, the majority of proteins having  $\beta$  sheets with excess hydrophilic surface exposure undergo the conformation changes in aqueous urea by preferentially solvating the polar residues.

However, it is important to note that it may not be true always that urea breaks  $\beta$  sheets and DMSO melts  $\alpha$  helices for all the proteins.<sup>27–29,46</sup> Our analyses here differ from the previous ones in this area. An additional merit of the present study is that it demonstrates and explains the origin of exceptions (as in ubiquitin), as a *complex interplay between the relative surface exposure of hydrophobic groups in different secondary structures and the polarity and hydrogen bonding ability of cosolvents*.

#### 4. SYSTEM SETUP AND SIMULATION DETAILS

As earlier mentioned in the text, we selected four well-characterized  $\alpha/\beta$  proteins, namely, (1) single immunoglobulin-binding domain protein G (PDB ID: 1GB1)<sup>51</sup> from group G Streptococcus, (2) chymotrypsin inhibitor 2 (PDB ID: 2CI2),<sup>52</sup> (3) IgG-binding domain of protein L (PDB ID: 2PTL),<sup>53</sup> and (4) human erythrocytic ubiquitin (PDB ID: 1UBQ).<sup>54</sup> We performed MD simulations of these four proteins in water–urea and water–DMSO binary mixtures varying urea and DMSO compositions by using the GROMACS package (version 4.0.5) with the Gromos96 force field (ffG43a1).<sup>55–57</sup> Numerous evaluations suggest that the GROMOS force field can be successfully applied for simulating several biomolecular systems including a number of solvents such as water, urea, chloroform, methanol, DMSO, carbon tetrachloride, and so forth. van Gunsteren and co-workers tested the compatibility of the molecular model for urea with the simple point charge model for liquid water for protein denaturation studies. They have validated MD simulation results to experimental data at 298 K as a function of urea mole fraction. In addition, thermodynamic properties, such as density, enthalpy of mixing, free enthalpy of urea hydration, and urea diffusion, show well agreement with the experimental values.<sup>58</sup> Similarly Oostenbrink and co-workers reported that the united atom model of DMSO combined with the GROMOS force field is reliable to produce any physical properties of liquid DMSO, including rotational correlation time, thermal expansion coefficient, isothermal compressibility, specific heat, excess Helmholtz free energy, static dielectric permittivity, shear viscosity, to name a few. All results were in good agreement with experiments.<sup>58</sup>

We performed standard MD simulations of time scale around 50 ns at different composition of urea and DMSO. We essentially practiced the protocol as mentioned by Rocco and co-workers.<sup>28,29</sup> To accelerate the unfolding process, for better sampling, and in order to avoid the traps in the path, we performed a number of MD simulations in water, urea, and DMSO at five different temperatures (300, 350, 400, 450, and 480 K). We find that, for temperatures of 300, 350, and 400 K, native structures of all the proteins taken were minimally perturbed. They essentially unfolded in water within the range of 450–480 K or above. However, at 400 K, addition of 8 M urea or 8 M DMSO greatly enhances the rate of unfolding of these proteins. Thus, the rate of enhancement of the unfolding process allowed us to compare several properties of four proteins in urea and DMSO solutions within the time scale of 50 ns. We monitored several parameters to investigate the different unfolding mechanisms experienced by these proteins under these specific conditions. It is important to note that the residual level secondary structural information for each protein was collected from their Protein Data Bank source files.<sup>51–54</sup>

In addition, to make composition-dependent binary mixtures, at first, we prepared water–urea and water–DMSO binary mixtures at various concentrations in cubic boxes, with sides of 3.0 nm. We used the SPC/E model for water molecules.<sup>59</sup> Methyl groups of DMSO were modeled as united atom within ffG43a1 force field.<sup>55–57</sup> After steepest descent energy minimization, each trajectory was propagated in an NVT ensemble and equilibrated for 2 ns. All the simulations in this study were done at 300 K and 1 bar pressure. The temperature was kept constant using the Nose–Hoover thermostat.<sup>60,61</sup> It was followed by an NPT equilibration for 20 ns using the

Parinello–Rahman barostat.<sup>62</sup> After preparing the binary solvents at various concentrations, the selected protein was dissolved in each of them and again followed the same procedure of energy minimization. A total of around 5000–6000 solvent molecules were taken. To further equilibrate the solvent before starting a full MD simulation, we hold the protein fixed while allowing the solvent to move around at constant temperature by performing position restrained MD for 5 ns. This allows the solvent to relax to a state that is natural for the current (native) conformation of the protein. Finally, production runs were performed for each system in an NVT ensemble. All the results were extracted from the 50 ns trajectory. The box size was enlarged to 6–6.5 nm to accommodate all the molecules. Periodic boundary conditions were applied, and nonbonded force calculations employed a grid system for neighbor searching.<sup>63</sup> Neighbor list generation was performed after every 10 steps using a cutoff of 0.9 nm. A cutoff radius of 1.2 nm was used for van der Waals' interaction. To calculate the electrostatic interactions, we used PME with a grid spacing of 0.12 nm and an interpolation order of 4.<sup>64–66</sup>

#### ■ ASSOCIATED CONTENT

##### ● Supporting Information

Figures showing conformational fluctuation of protein G and the fraction of native contact ( $\eta$ ) dynamics. This material is available free of charge via the Internet at <http://pubs.acs.org>.

#### ■ AUTHOR INFORMATION

##### Corresponding Author

\*Email: [bbagchi@sscu.iisc.ernet.in](mailto:bbagchi@sscu.iisc.ernet.in).

##### Notes

The authors declare no competing financial interest.

#### ■ ACKNOWLEDGMENTS

We thank Rikhia Ghosh for many useful discussions. This work was supported in parts by grants from DST, India. B.B. acknowledges support from JC Bose fellowship from DST, India.

#### ■ REFERENCES

- (1) Bagchi, B. *Water in Biological and Chemical Processes: From Structure and Dynamics to Function*; Cambridge University Press, London, U.K., 2013.
- (2) Levinthal, C. Are There Pathways for Protein Folding? *J. Chim. Phys.* **1968**, *65*, 44–45.
- (3) Levinthal, C. How to Fold Graciously. In *Mossbauer Spectroscopy in Biological System*, Proceedings of a Meeting Held at Allerton House, Monticello, IL, March 17 and 18, 1969; De-Brunner, P., Tsibris, J., Munck, E., Eds.; University of Illinois Press: Urbana, IL, 1969; pp 22–24.
- (4) Zwanzig, R.; Szabo, A.; Bagchi, B. Levinthal's Paradox. *Proc. Natl. Acad. Sci. U.S.A.* **1992**, *89*, 20–22.
- (5) Bryngelson, J. D.; Wolynes, P. G. Intermediates and Barrier Crossing in a Random Energy Model (with Applications to Protein Folding). *J. Phys. Chem.* **1989**, *93*, 6902–6915.
- (6) Leopold, P. E.; Montal, M.; Onuchic, J. N. Protein Folding Funnels: A Kinetic Approach to the Sequence-Structure Relationship. *Proc. Natl. Acad. Sci. U.S.A.* **1992**, *89*, 8721–8725.
- (7) Bryngelson, J. D.; Onuchic, J. N.; Socci, N. D.; Wolynes, P. G. Funnels, Pathways, and the Energy Landscape of Protein Folding: A Synthesis. *Proteins: Struct., Funct., Genet.* **1995**, *21*, 167–195.
- (8) Onuchic, J. N.; Wolynes, P. G. Theory of Protein Folding. *Curr. Opin. Struct. Biol.* **2004**, *14*, 70–75.

- (9) Chan, H. S.; Dill, K. A. Polymer Principles in Protein Structure and Stability. *Annu. Rev. Biophys. Biophys. Chem.* **1991**, *20*, 447–490.
- (10) Dill, K.; Chan, H. S. From Levinthal to Pathways to Funnels. *Nat. Struct. Biol.* **1997**, *4*, 10–19.
- (11) Chan, H. S.; Dill, K. A. Protein Folding in the Landscape Perspective: Chevron Plots and Non-Arrhenius Kinetics. *Proteins* **1998**, *30*, 2–33.
- (12) Karplus, M. The Levinthal Paradox: Yesterday and Today. *Folding Des.* **1997**, *2*, S69–S75.
- (13) Sali, A.; Shakhnovich, E.; Karplus, M. How Does a Protein Fold? *Nature* **1994**, *369*, 248–251.
- (14) Karplus, M.; Weaver, D. L. Protein-Folding Dynamics. *Nature* **1976**, *260*, 404–406.
- (15) Honeycutt, J. D.; Thirumalai, D. Metastability of the Folded States of Globular Proteins. *Proc. Natl. Acad. Sci. U.S.A.* **1990**, *87*, 3526–3529.
- (16) Wolynes, P. G.; Onuchic, J. N.; Thirumalai, D. Navigating the Folding Routes. *Science* **1995**, *267*, 1619–1620.
- (17) Wales, D. J. The Energy Landscape as a Unifying Theme in Molecular Science. *Philos. Trans. R. Soc., A* **2005**, *363*, 357–377.
- (18) Wales, D. J.; Bogdan, T. V. Potential Energy and Free Energy Landscapes. *J. Phys. Chem. B* **2006**, *110*, 20765–20776.
- (19) Carr, J. M.; Wales, D. J. Global Optimization and Folding Pathways of Selected  $\alpha$ -Helical Proteins. *J. Chem. Phys.* **2005**, *123*, 23490.
- (20) Baldwin, R. L. The Nature of Protein Folding Pathways: The Classical versus the New View. *J. Biomol. NMR* **1995**, *5*, 103–109.
- (21) Baldwin, R. L. Competing Unfolding Pathways. *Nat. Struct. Biol.* **1997**, *4*, 965–966.
- (22) Fersht, A. R.; Itzhaki, L. S.; elMasry, N. F.; Matthews, J. M.; Otzen, D. E. Single versus Parallel Pathways of Protein Folding and Fractional Formation of Structure in the Transition State. *Proc. Natl. Acad. Sci. U.S.A.* **1994**, *91*, 10426–10429.
- (23) Fersht, A. R. Optimization of Rates of Protein Folding: The Nucleation-Condensation Mechanism and Its Implications. *Proc. Natl. Acad. Sci. U.S.A.* **1995**, *92*, 10869–10873.
- (24) Oliveberg, M.; Tan, Y. J.; Fersht, A. R. Negative Activation Enthalpies in the Kinetics of Protein Folding. *Proc. Natl. Acad. Sci. U.S.A.* **1995**, *92*, 8926–8929.
- (25) Pande, V. S.; Grosberg, A. Yu.; Tanaka, T.; Rokhsar, D. S. Pathways for Protein Folding: Is a New View Needed? *Curr. Opin. Struct. Biol.* **1998**, *8*, 68–79.
- (26) Lindorff-Larsen, K.; Piana, S.; Dror, R. O.; Shaw, D. E. How Fast-Folding Proteins Fold. *Science* **2011**, *334*, 517–520.
- (27) Bennion, B. J.; Daggett, V. Counteraction of Urea-Induced Protein Denaturation by Trimethylamine N-Oxide: A Chemical Chaperone at Atomic Resolution. *Proc. Natl. Acad. Sci. U.S.A.* **2003**, *100*, 5142–5147.
- (28) Camilloni, C.; Rocco, A. G.; Eberini, I.; Gianazza, E.; Broglia, R. A.; Tiana, G. Urea and Guanidinium Chloride Denature Protein L in Different Ways in Molecular Dynamics Simulations. *Biophys. J.* **2008**, *94*, 4654–61.
- (29) Rocco, A. G.; Mollica, L.; Ricchiuto, P.; Baptista, A. M.; Gianazza, E.; Eberini, I. Characterization of the Protein Unfolding Processes Induced by Urea and Temperature. *Biophys. J.* **2008**, *94*, 2241–51.
- (30) Maity, H.; Maity, M.; Englander, S. W. How Cytochrome C Folds, and Why: Submolecular Foldon Units and Their Stepwise Sequential Stabilization. *J. Mol. Biol.* **2004**, *343*, 223–233.
- (31) Krishna, M. M. G.; Maity, H.; Rumbley, J. N.; Lin, Y.; Englander, S. W. Order Steps in the Cytochrome C Folding Pathway: Evidence for a Sequential Stabilization Mechanism. *J. Mol. Biol.* **2006**, *359*, 1410–1419.
- (32) Krishna, M. M. G.; Englander, S. W. A Unified Mechanism for Protein Folding: Predetermined Pathways with Optional Errors. *Protein Sci.* **2007**, *16*, 449–464.
- (33) Kim, S.; Chung, J. K.; Kwak, K.; Bren, K. L.; Bagchi, B.; Fayer, M. D. Native and Unfolded Cytochrome *c* – Comparison of Dynamics Using 2D-IR Vibrational Echo Spectroscopy. *J. Phys. Chem. B* **2008**, *112*, 10054–10063.
- (34) Frank, H. S.; Franks, F. Structural Approach to the Solvent Power of Water for Hydrocarbons; Urea as a Structure Breaker. *J. Chem. Phys.* **1968**, *48*, 4746–4757.
- (35) Tobi, D.; Elber, R.; Thirumalai, D. The Dominant Interaction between Peptide and Urea Is Electrostatic in Nature: A Molecular Dynamics Simulation Study. *Biopolymers* **2003**, *68*, 359–369.
- (36) O'Brien, E. P.; Dima, R. I.; Brooks, B.; Thirumalai, D. Interactions between Hydrophobic and Ionic Solutes in Aqueous Guanidinium Chloride and Urea Solutions: Lessons for Protein Denaturation Mechanism. *J. Am. Chem. Soc.* **2007**, *129*, 7346–7353.
- (37) Das, A.; Mukhopadhyay, C. Urea-Mediated Protein Denaturation: A Consensus View. *J. Phys. Chem. B* **2009**, *113*, 12816–12824.
- (38) Zhou, R.; Li, J.; Hua, L.; Yang, Z.; Berne, B. J. Comment on “Urea-Mediated Protein Denaturation: A Consensus View”. *J. Phys. Chem. B* **2011**, *115*, 1323–1328.
- (39) Hua, L.; Zhou, R.; Thirumalai, D.; Berne, B. J. Urea Denaturation by Stronger Dispersion Interactions with Proteins than Water Implies a 2-Stage Unfolding. *Proc. Natl. Acad. Sci. U.S.A.* **2008**, *105*, 16928–16933.
- (40) Caflisch, A.; Karplus, M. Structural Details of Urea Binding to Barnase: A Molecular Dynamics Analysis. *Structure* **1999**, *7*, 477–488.
- (41) Roy, S.; Jana, B.; Bagchi, B. Dimethyl Sulfoxide Induced Structural Transformations and Non-Monotonic Concentration Dependence of Conformational Fluctuation around Active Site of Lysozyme. *J. Chem. Phys.* **2012**, *136*, 115103/1–10.
- (42) Jackson, M.; Mantsch, H. H. Beware of Proteins in DMSO. *Biochim. Biophys. Acta* **1991**, *1078*, 231–5.
- (43) Huang, P.; Dong, A.; Caughey, W. S. Effects of Dimethyl Sulfoxide, Glycerol, and Ethylene Glycol on Secondary Structures of Cytochrome *c* and Lysozyme as Observed by Infrared Spectroscopy. *J. Pharm. Sci.* **1995**, *84*, 387–392.
- (44) Roy, S.; Bagchi, B. Chemical Unfolding of Chicken Villin Headpiece in Aqueous Dimethyl Sulfoxide Solution: Cosolvent Concentration Dependence, Pathway, and Microscopic Mechanism. *J. Phys. Chem. B* **2013**, *117*, 4488–4502.
- (45) Tretyakova, T.; Shushanyan, M.; Partskhaladze, T.; Makharadze, M.; van Eldik, R.; Khoshtariya, D. E. Simplicity within the Complexity: Bilateral Impact of DMSO on the Functional and Unfolding Patterns of  $\alpha$ -Chymotrypsin. *Biophys. Chem.* **2013**, *175*–176, 17–27.
- (46) Batista, A. N.; Batista, J. M., Jr.; Bolzani, V. S.; Furlan, M.; Blanch, E. W. Selective DMSO-Induced Conformational Changes in Proteins from Raman Optical Activity. *Phys. Chem. Chem. Phys.* **2013**, *15*, 20147–20152.
- (47) Piana, S.; Lindorff-Larsen, K.; Shaw, D. E. Atomic-Level Description of Ubiquitin Folding. *Proc. Natl. Acad. Sci. U.S.A.* **2013**, *110*, 5915–5920.
- (48) Larios, E.; Yang, W. Y.; Schulten, K.; Gruebele, M. A Similarity Measure for Partially Folded Proteins: Application to Unfolded and Native-like Conformation Fluctuations. *Chem. Phys.* **2004**, *307*, 217–225.
- (49) Yang, W. Y.; Pitera, J. W.; Swope, W. C.; Gruebele, M. Heterogeneous Folding of the Trpzip Hairpin: Full Atom Simulation and Experiment. *J. Mol. Biol.* **2004**, *336*, 241–251.
- (50) Larios, E.; Li, J. S.; Schulten, K.; Kihara, H.; Gruebele, M. Multiple Probes Reveal a Native-like Intermediate during Low-Temperature Refolding of Ubiquitin. *J. Mol. Biol.* **2004**, *340*, 115–125.
- (51) Gronenborn, A. M.; Filpula, D. R.; Essig, N. Z.; Achari, A.; Whitlow, M.; Wingfield, P. T.; Clore, G. M. A Novel, Highly Stable Fold of the Immunoglobulin Binding Domain of Streptococcal Protein G. *Science* **1991**, *253*, 657–661.
- (52) McPhalen, C. A.; James, M. N. Crystal and Molecular Structure of the Serine Proteinase Inhibitor CI-2 from Barley Seeds. *Biochemistry* **1987**, *26*, 261–269.
- (53) Wikstrom, M.; Drakenberg, T.; Forsen, S.; Sjobring, U.; Bjorck, L. Three-Dimensional Solution Structure of an Immunoglobulin Light Chain-Binding Domain of Protein L. Comparison with the IgG-Binding Domains of Protein G. *Biochemistry* **1994**, *33*, 14011–14017.



- (54) Vijay-Kumar, S.; Bugg, C. E.; Cook, W. J. Structure of Ubiquitin Refined at 1.8 Å Resolution. *J. Mol. Biol.* **1987**, *194*, 531–544.
- (55) Oostenbrink, C.; Villa, A.; Mark, A. E.; van Gunsteren, W. F. A Biomolecular Force Field Based on the Free Enthalpy of Hydration and Solvation: The GROMOS Force-Field Parameter Sets 53A5 and 53A6. *Comput. Chem.* **2004**, *25*, 1656–1676.
- (56) Liu, H. Y.; Müller-Plathe, F.; van Gunsteren, W. F. A Force Field for Liquid Dimethyl Sulfoxide and Physical Properties of Liquid Dimethyl Sulfoxide Calculated Using Molecular Dynamics Simulation. *J. Am. Chem. Soc.* **1995**, *117*, 4363–4366.
- (57) Geerke, D. P.; Oostenbrink, C.; van der Vegt, N. F. A.; van Gunsteren, W. F. An Effective Force Field for Molecular Dynamics Simulations of Dimethyl Sulfoxide and Dimethyl Sulfoxide–Water Mixtures. *J. Phys. Chem. B* **2004**, *108*, 1436–1445.
- (58) Smith, L. J.; Berendsen, H. J. C.; van Gunsteren, W. F. Computer Simulation of Urea–Water Mixtures: A Test of Force Field Parameters for Use in Biomolecular Simulation. *J. Phys. Chem. B* **2004**, *108*, 1065–1071.
- (59) Berendsen, H. J. C.; Grigera, J. R.; Straatsma, T. P. The Missing Term in Effective Pair Potentials. *J. Phys. Chem.* **1987**, *89*, 6269–6271.
- (60) Hoover, W. G. Canonical Dynamics: Equilibrium Phase-Space Distributions. *Phys. Rev. A* **1985**, *31*, 1695–1697.
- (61) Nose, S. A Unified Formulation of the Constant Temperature Molecular Dynamics Methods. *J. Chem. Phys.* **1984**, *81*, 511–519.
- (62) Parinello, M.; Rahman, A. Polymorphic Transitions in Single Crystals: A New Molecular Dynamics Method. *J. Appl. Phys.* **1981**, *52*, 7182–7190.
- (63) Frenkel, D.; Smit, B. *Understanding Molecular Simulation: From Algorithms to Applications*, 2nd ed.; Academic Press: San Diego, CA, 2002.
- (64) Roy, S.; Banerjee, S.; Biyani, N.; Jana, B.; Bagchi, B. Theoretical and Computational Analysis of Static and Dynamic Anomalies in Water–DMSO Binary Mixture at Low DMSO Concentrations. *J. Phys. Chem. B* **2010**, *115*, 685–692.
- (65) Banerjee, S.; Roy, S.; Bagchi, B. Enhanced Pair Hydrophobicity in Water–DMSO Binary Mixture at Low DMSO Concentration. *J. Phys. Chem. B* **2010**, *114*, 12875–12882.
- (66) Roy, S.; Bagchi, B. Solvation Dynamics of Tryptophan in Water–Dimethyl Sulfoxide Binary Mixture: In Search of Molecular Origin of Composition Dependent Multiple Anomalies. *J. Chem. Phys.* **2013**, *139*, 034308/1–10.